An embedded Cartesian scheme for the Navier-Stokes equations

Jean-Pierre Croisille

Département de Mathématiques

Institut Elie Cartan de Lorraine - UMR CNRS 7502

Univ. Lorraine - Metz, France

March 22, 2019

Joint work with
Matania Ben-Artzi, Hebrew Univ., Jerusalem, Israel
Dalia Fishelov, Afeka College of Eng., Tel Aviv, Israel
Guy Katriel, ORT Braude College, Karmiel, Israel

Outline

- The streamfunction form of the Navier-Stokes (NS) equation
- A compact scheme for the biharmonic problem in 1D and 2D
- Extending compact approximation to irregular domains by Cartesian embedding
- The NS problem in an ellipse
- Eigenproblems for Δ^2

Navier-Stokes equations in 2D

NS equations in primitive variables

Velocity: $\boldsymbol{v}(t,\mathbf{x})$, Pressure: $p(t,\mathbf{x})$, $\mathbf{x}=(x,y)$, Source term: $\underline{\mathsf{f}}=(f_1,f_2)$

$$\begin{cases} \partial_t \boldsymbol{v} + \boldsymbol{v}.\nabla \boldsymbol{v} + \nabla p - \nu\Delta \boldsymbol{v} = \underline{\mathsf{f}}, \quad \nu > 0 \\ \operatorname{div} \boldsymbol{v} = 0 \end{cases} \tag{1}$$

Vorticity $\omega = \operatorname{curl} \boldsymbol{v}$

Equation for $\omega(t,\mathbf{x})$:

$$\partial_t\omega + \boldsymbol{v}.\nabla\omega - \nu\Delta\omega = \partial_x f_2 - \partial_y f_1 \tag{2}$$

Navier-Stokes equation in pure streamfunction Formulation (Lagrange 1768)

Let $\boldsymbol{v}(t, \mathbf{x}) = (-\partial_y \psi, \partial_x \psi) = \nabla^\perp \psi$, where ψ is the streamfunction. The equation for ω is expressed as

$$\partial_t(\Delta\psi) + (\nabla^\perp \psi) \cdot \nabla(\Delta\psi) - \nu \Delta^2 \psi = \partial_x f_2 - \partial_y f_1, \quad \text{in } \Omega. \qquad (3)$$

Boundary and initial conditions:

- $$\psi(x, y, t) = \frac{\partial \psi}{\partial n}(x, y, t) = 0, \quad (x, y) \in \partial\Omega \qquad (4)$$
- $$\psi_0(x, y) = \psi(x, y, t)|_{t=0}, \quad (x, y) \in \Omega \qquad (5)$$

No need for vorticity boundary conditions.

NS equation in pure streamfunction form, cont.

- The streamfunction ψ plays the role of a ”vector potential” of the velocity field.
- Once ψ is known, the velocity $\boldsymbol{v}$ and pressure force ∇p are obtained by:

$$\begin{cases} \boldsymbol{v} = \nabla^{\perp}\psi, \\ \nabla p = -\Big(\partial_t \Delta\psi + \nabla^{\perp}\psi . \Delta(\nabla^{\perp}\psi) - \nu\nabla^{\perp}(\Delta\psi)\Big) \end{cases} \tag{6}$$

General Goals

- Discretize the 2D NS equation in streamfunction form with a high order finite difference scheme in space and time.
- Treat irregular boundaries by direct embedding in a Cartesian grid.
- Investigate numerically complicated patterns of the 2D NS equation.

Discrete operator δ_x^4

Approximating biharmonic problems is the main issue.

- 4th order ODE in $[0,1]$

$$\begin{cases} \frac{d^4}{dx^4}\psi(x) = f(x), \;\; 0 < x < 1 \\ \psi(0) = 0, \; \psi(1) = 0, \; \psi'(0) = 0, \; \psi'(1) = 0. \end{cases} \tag{7}$$

- Lay out a uniform grid $x_0, x_1, ..., x_N$ where $x_j = jh$ and $h = 1/N$.
- Discrete problem

$$\begin{cases} \delta_x^4 \psi_j = f(x_j), 1 \le j \le N-1 \\ \psi_0 = \psi_N = \psi_{x,0} = \psi_{x,N} = 0 \end{cases} \tag{8}$$

- How is defined the finite difference discrete operator δ_x^4 ?

Discrete operator δ_x^4 via Taylor series

- Formula for $\delta_x^4 \psi_j$:

$$\delta_x^4 \psi_j = \frac{12}{h^2}\Big(\underbrace{\frac{\psi_{x,j+1} - \psi_{x,j-1}}{2h}}_{(I)} - \underbrace{\frac{\psi_{j+1} + \psi_{j-1} - 2\psi_j}{h^2}}_{(II)} \Big) \quad (9)$$

- The term (II) is the three point finite difference for $\frac{d^2}{dx^2}\psi(x_j)$

$$\delta_x^2 \psi_j = \frac{\psi_{j+1} + \psi_{j-1} - 2\psi_j}{h^2} \quad (10)$$

- The term (I) involves the approximate derivative $\psi_{x,j} \simeq \frac{d}{dx}u(x_j)$ solution of

$$\frac{1}{6}\psi_{x,j-1} + \frac{2}{3}\psi_{x,j} + \frac{1}{6}\psi_{x,j+1} = \frac{\psi_{j+1} - \psi_{j-1}}{2h} \quad (11)$$

- Subtracting (10) from $\delta_x \psi_{x,j}$ and scaling gives

$$\delta_x^4 \psi_j = \frac{d^4}{dx^4}\psi(x_j) + O(h^2), \;\; 2 \le j \le N-2 \quad (12)$$

Discrete operator δ_x^4 via Taylor series, cont.

Fourth-order accuracy

Surprinsingly, δ_x^4 is fourth order accurate !

$$\delta_x^4 \psi_j - \left(\frac{d^4\psi}{dx^4}\right)_j = -\frac{h^4}{720}\left(\frac{d^8 u}{dx^8}\right)_j + O(h^6) \tag{13}$$

Discrete operator δ_x^4 by Lagrange interpolation

- Polynomial $Q(x)$:

$$Q(x) = a_0 + a_1(x - x_j) + a_2(x - x_j)^2 + a_3(x - x_j)^3 + a_4(x - x_j)^4 \quad (14)$$

- Define $Q(x)$ by the 5 interpolation equations at points x_{j-1}, x_j and x_{j+1}:

$$\begin{cases} Q(x_{j-1}) = \psi_{j-1}, \ \ Q(x_j) = \psi_j, \ \ Q(x_{j+1}) = \psi_{j+1}, \\ Q'(x_{j-1}) = \psi_{x,j-1}, \ \ Q'(x_{j+1}) = \psi_{x,j+1} \end{cases} \quad (15)$$

- $\delta_x^4 \psi_j$ is obtained by

$$\delta_x^4 \psi_j = 24 a_4 \quad (16)$$

Consistency of δ_x^4

Proposition

Suppose that $\psi(x)$ is a smooth function on $[0,1]$. Then, with $\sigma_x = I + \frac{h^2}{6}\delta_x^2$ and u^*, the restriction of $u(x)$ to the grid, the following holds:

- *Fourth order accuracy at internal points*

$$|\sigma_x\big(\delta_x^4\psi_j^* - (\psi^{(4)})^*(x_j)\big)| \leq Ch^4\|\psi^{(8)}\|_{L^\infty}, \quad 2 \leq i \leq N-2. \quad (17)$$

- *At near boundary points $j=1$ and $j=N-1$, the fourth order accuracy of (17) drops to first order*

$$|\sigma_x\big(\delta_x^4\psi_j^* - (\psi^{(4)})^*(x_j)\big)| \leq Ch\|\psi^{(5)}\|_{L^\infty}, \quad j = 1, N-1. \quad (18)$$

Optimal error convergence for δ_x^4

Theorem

Let $\tilde{\psi}$ be the approximate solution of the biharmonic problem and let ψ be the exact solution and ψ^* its evaluation at grid points. The error $\mathbf{e} = \tilde{\psi} - \psi^* = \delta_x^{-4} f^* - (\partial_x^{-4} f)^*$ satisfies

$$\max_{1 \leq j \leq N-1} |\mathbf{e}_j| \leq Ch^4, \quad |\mathbf{e}|_h \leq Ch^4, \tag{19}$$

where C depends only on f.

"Optimality" of $(\delta_x^4)^{-1}$

Theorem

Let $(\psi_j)_{1\leq j\leq N-1}$ *be the solution of*

$$\delta_x^4\psi_j = f(x_j),\ \ 1\leq j\leq N-1,\ \ \psi_0=\psi_N=0 \tag{20}$$

Then ψ *is given by*

$$\psi_j = h\sum_{i=1}^{N-1} K(x_i,x_j)(\delta_x^4\psi)_i \tag{21}$$

where $K(x,y)$ *is the Green function of*

$$\frac{d^4}{dx^4}\psi = f,\ \ 0<x<1,\ \ \psi(0)=\psi(1)=\frac{d\psi}{dx}(0)=\frac{d\psi}{dx}(1)=0 \tag{22}$$

$$K(x,y)=\begin{cases}\dfrac{1}{6}(1-x)^2y^2(2x(1-y)+x-y), & y<x\\ \dfrac{1}{6}(1-y)^2x^2(2y(1-x)+y-x), & x<y\end{cases} \tag{23}$$

Numerical results for time-dependent 1D-Kuramoto-Sivashinsky Eqn.

Consider the Kuramoto–Sivashinsky equation

$$\begin{aligned} &\partial_t u = -\partial_x^4 u - \partial_x^2 u - u\partial_x u + f, \quad -30 < x < 30, \quad t > 0, \\ &u(0,t) = \partial_x u(0,t) = 0 = u(1,t) = \partial_x u(1,t) = 0. \end{aligned} \tag{24}$$

Pick up the exact solution $u(x,t)$ as in Xu and Shu (2006)

$$u(x,t) = c+(15/19)\sqrt{11/19}(-9\tanh(k(x-ct-x_0))+11\tanh^3(k(x-ct-x_0)). \tag{25}$$

Here $c = -0.1, k = 0.5\sqrt{11/19}$ and $x_0 = -10$.

Mesh	$N = 241$	Rate	$N = 481$	Rate	$N = 961$
$\|\mathbf{e}\|_h$	3.2873(-4)	3.99	2.0752(-5)	4.00	1.2984(-6)
$\|\mathbf{e}_x\|_h$	2.9822(-4)	3.95	1.9332(-5)	3.98	1.2246(-6)

Table: KS equation (24), where $T_{final} = 1$ and $\Delta t = h^2$.

Numerical results for time-dependent problems in 1D-Kuramuto-Sivashinsky Eqn., cont.

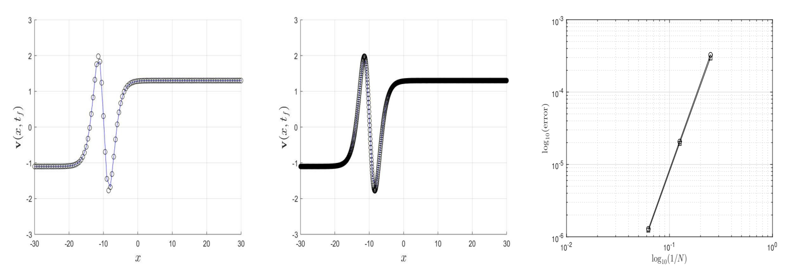

Figure: KS equation: Exact solution (solid line) and computed solution (circles) with $N = 121$ (left) and $N = 961$ (center) The convergence rate is shown in the right panel for u (circles) and $\frac{\partial u}{\partial x}$ (squares).

Discrete Biharmonic in a square

Enhanced three point operator $\tilde{\delta}_x^2 \psi_j$

$$\tilde{\delta}_x^2 \psi_j := \delta_x^2 \psi_j - \frac{h^2}{12} \delta_x^4 \psi_j = \psi''(x_j) + O(h^4) \quad (26)$$

Two-dimensional discrete Biharmonic

$$\Delta_h^2 = \delta_x^4 + \delta_y^4 + 2\tilde{\delta}_x^2 \tilde{\delta}_y^2 \quad (27)$$

$$\Delta_h^2 u_{i,j} - (\Delta^2 u)_{i,j} = -h^4 \Big(\frac{1}{720} (\partial_x^8 + \partial_y^8) u_{i,j} + \frac{1}{72} (\partial_x^4 \partial_y^4 u)_{i,j} - \frac{1}{180} (\partial_x^2 \partial_y^6 + \partial_x^6 \partial_y^2) u_{i,j} \Big) + O(h^6) \quad (28)$$

FFT solver

Discrete problem $(\Delta_h^2 \tilde{\psi})_{i,j} = f_{i,j}$ solvable by FFT. Typical computing time: 1 sec to solve a 512×512 problem on a laptop.

Semi-discrete Navier-Stokes equations in a square

- NS equation with unknown $\psi(t,\mathbf{x})$:

$$\partial_t \Delta\psi(t,\mathbf{x}) + \nabla^{\perp}\psi(t,\mathbf{x}).(\Delta\nabla\psi(t,\mathbf{x})) - \nu\Delta^2\psi(t,\mathbf{x}) = \mathbf{f}(t,\mathbf{x}) \quad (29)$$

- Discrete version with unknown $\tilde{\psi}(t) = \tilde{\psi}_{i,j}(t)$:

$$\frac{d}{dt}\Delta_h\widetilde{\psi} + \nabla_h^{\perp}\widetilde{\psi}\cdot(\Delta_h\nabla_h\widetilde{\psi}) - \nu\Delta_h^2\widetilde{\psi} = \mathbf{f}^*(t,.) \quad (30)$$

Convergence of the semi-discrete scheme

Theorem

Define the error $e(t)$ *as* $e(t) = \widetilde{\psi} - \psi$. *Let* $T > 0$. *Then there exist constants* $C, h_0 > 0$, *depending possibly on* T, ν *and the exact solution* ψ, *such that, for all* $0 \leq t \leq T$,

$$|\delta_x^+ e|_h^2 + |\delta_y^+ e|_h^2 \leq Ch^3 \quad , \quad 0 < h \leq h_0. \tag{31}$$

where

$$\delta_x^+ \psi_{i,j} = \frac{\psi_{i+1,j} - \psi_{i,j}}{h}, \quad \delta_y^+ \psi_{i,j} = \frac{\psi_{i,j+1} - \psi_{i,j}}{h} \tag{32}$$

Time Discretization: IMEX scheme

- Consider

$$\frac{d\psi(t)}{dt} = \underbrace{F_c(\psi(t))}_{convection} + \underbrace{F_d(\psi(t))}_{diffusion} \tag{33}$$

  An IMEX time stepping scheme is
  - Explicit for $F_c(\psi)$.
  - Implicit for $F_d(\psi)$
- Typical IMEX scheme for NS equations:

$$\begin{cases} \dfrac{(\tilde{\Delta}_h\psi_{i,j})^{n+1/2} - (\tilde{\Delta}_h\psi_{i,j})^n}{\Delta t/2} = -\tilde{C}_h(\psi^n)_{i,j} + \dfrac{\nu}{2}\Big(\tilde{\Delta}_h^2\psi_{i,j}^{n+1/2} + \tilde{\Delta}_h^2\psi_{i,j}^n\Big) \\ \dfrac{(\tilde{\Delta}_h\psi_{i,j})^{n+1} - (\tilde{\Delta}_h\psi_{i,j})^n}{\Delta t} = -\tilde{C}_h(\psi^{n+1/2})_{i,j} + \dfrac{\nu}{2}\Big(\tilde{\Delta}_h^2\psi_{i,j}^{n+1} + \tilde{\Delta}_h^2\psi_{i,j}^n\Big) \end{cases} \tag{34}$$

- Only the discrete Laplacian and biharmonic operators, which are approximated by a compact scheme, have to be inverted at each step.

Irregular domain embedded in a Cartesian grid

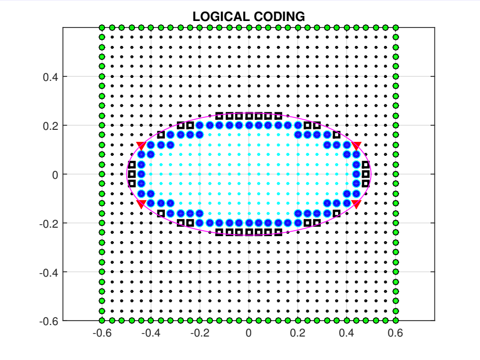

Figure: Ellipse $4x^2 + 16y^2 = 1$ embedded in $[-0.6, 0.6] \times [-0.6, 0.6]$. with Cartesian grid 30×30.

- RED TRIANGLES = Boundary points
- BLACK OPEN SQUARES = Edge points
- DARK BLUE CIRCLES = Irregular calculated points.

Near boundary stencil

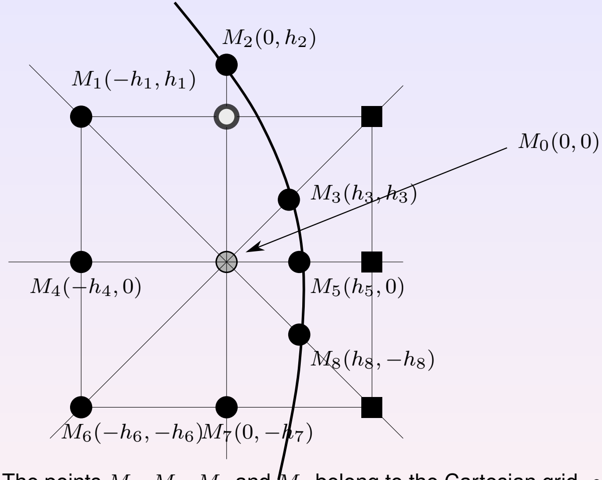

Figure: • The points M_1, M_4, M_6 and M_7 belong to the Cartesian grid. • The points M_2, M_3, M_5 and M_8 belong to the boundary of the domain. • The edge point above M_0 is marked with an open circle.

Polynomial space of dimension 19

The polynomial $P_{\mathbf{M_0}}(x,y)$ is uniquely determined. It belongs to a polynomial space of dimension 19.

$$P_{\mathbf{M_0}}(x,y) = \sum_{p=1}^{19} a_p l_p(x,y), \tag{35}$$

where the $l_p(x,y)$ are

$$\begin{cases} l_1(x,y) = 1, \\ l_2(x,y) = x, \;\; l_3(x,y) = x^2, \;\; l_4(x,y) = x^3, \\ l_5(x,y) = x^4, \;\; l_6(x,y) = x^5, \\ l_7(x,y) = y, \;\; l_8(x,y) = y^2, \;\; l_9(x,y) = y^3, \\ l_{10}(x,y) = y^4, \;\; l_{11}(x,y) = y^5, \\ l_{12}(x,y) = xy, \\ l_{13}(x,y) = xy(x+y), \;\; l_{14}(x,y) = xy(x-y), \\ l_{15}(x,y) = xy(x+y)^2, \;\; l_{16}(x,y) = xy(x-y)^2, \\ l_{17}(x,y) = xy(x+y)^3, \;\; l_{18}(x,y) = xy(x-y)^3, \\ l_{19}(x,y) = x^2y^2(x^2+y^2). \end{cases} \tag{36}$$

Lagrange-Hermite Collocation scheme

Design of the Compact Embedded Scheme

The discrete Biharmonic $\Delta_{\mathbf{h}}^2\psi$, at $\mathbf{M_0} = (0,0)$ is

$$\Delta_{\mathbf{h}}^2\widetilde{\psi}(\mathbf{M_0}) = \Delta^2 P_{\mathbf{M_0}}(0,0). \quad (37)$$

$\Delta^2\psi = f$ in a star shaped domain

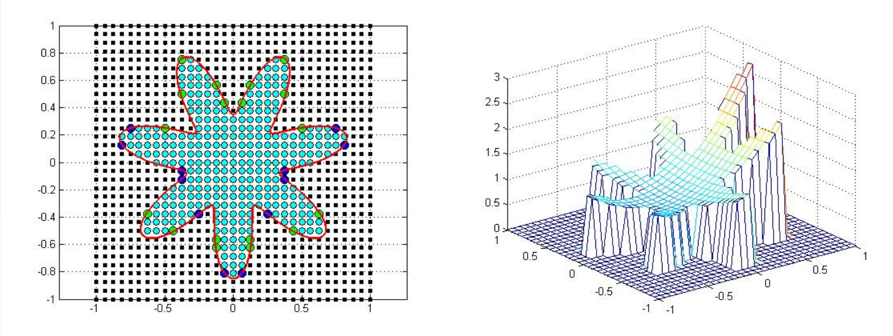

Figure: Seven branches star shaped domain embedded in a 33×33 grid. Left: domain and grid. Right: approximate solution corresponding to $\psi_{\text{ex}}(x, y) = x^2 + y^2 + e^x \cos(y)$.

- BLUE CIRCLES: Boundary points
- GREEN CIRCLES: Edge points.

3 and 5 branches star shaped domain: convergence rate

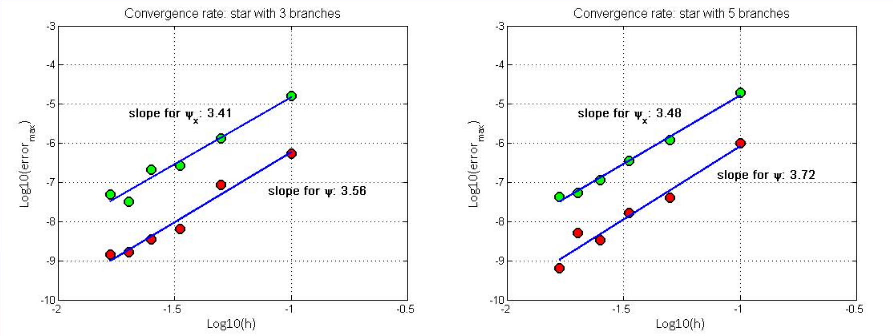

Figure: Linear regression of the convergence rate for $\|\psi - \psi_{\mathrm{ex}}\|_\infty$ and $\|\psi_x - \psi_{x,\mathrm{ex}}\|_\infty$ with $\psi_{\mathrm{ex}} = (x, y) = x^2 + y^2 + e^x \cos(y)$. The 6 points correspond to the 6 grids 10×10, 20×20, 30×30, 40×40, 50×50 and 60×60.

Navier-Stokes equation in an ellipse

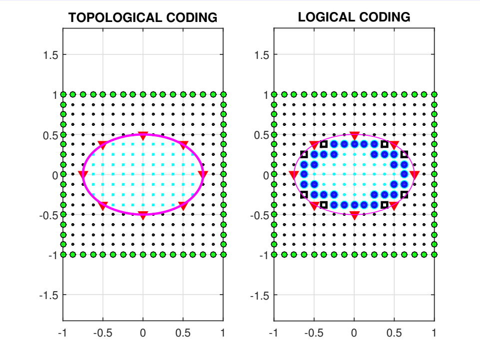

Figure: The ellipse $\frac{x^2}{0.5^2} + \frac{y^2}{0.25^2} \leq 1$

- LEFT: topological coding with 3 categories: Exterior, boundary and internal points.
- RIGHT: logical coding with 5 categories: Exterior, Boundary, Edge, Interior irregular and Interior regular calculated points.

The Exact and Calculated solution for the ellipse

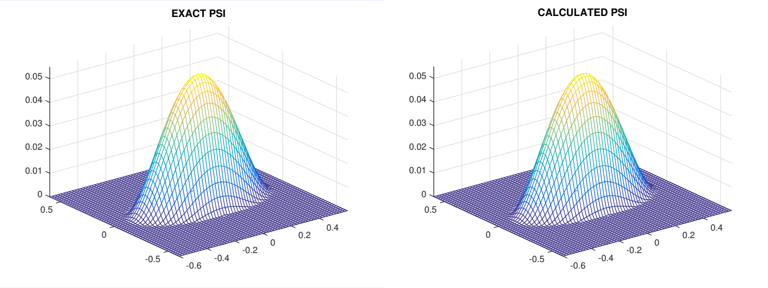

Figure: Ellipse embedded in a 60×60 Cartesian grid. NS for $\psi = (x^2 + 4y^2 - 0.25)^2 \cos(t)$ in the ellipse $4x^2 + 16y^2 \leq 1$: Exact and calculated solutions at final time $t_f = 0.5$.

Errors for ψ and $\partial_y \psi$ in an ellipse

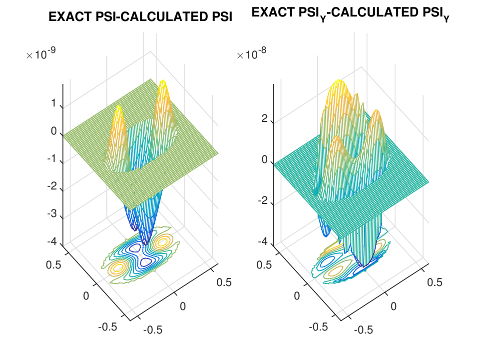

Figure: Error in ψ and ψ_y at $t_f = 0.5$, $\nu = 0.001$, 60×60 grid for the ellipse $4x^2 + 16y^2 \leq 1$.

Convergence rates for the ellipse

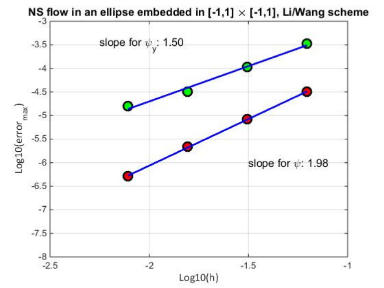

(a) Li and Wang embedded scheme

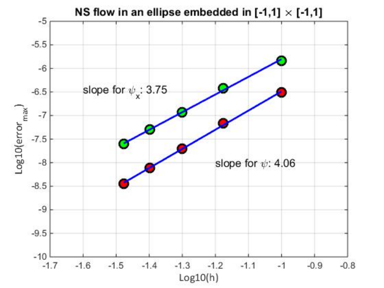

(b) Present scheme

Figure: Regression lines for the Li and Wang test case. Left: Li and Wang convergence rate with $N = 32, 64, 128, 256$. Right: Present scheme with $N = 20, 30, 40, 50, 60$. Note that the accuracy with $N = 20$ on the right is better than the accuracy with $N = 256$ on the left.

Consistency of the accuracy under grid rotation

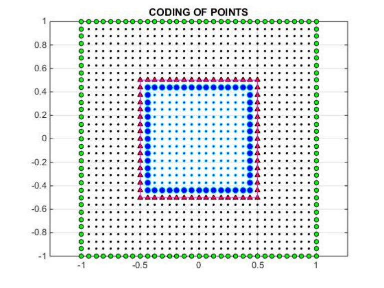

(a) Coding of Points $\theta = 0$

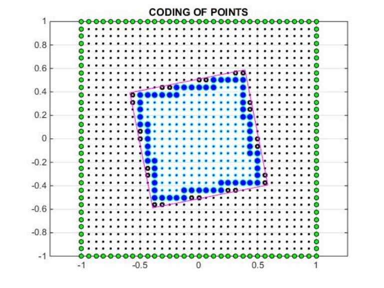

(b) Coding of Points $\theta = \pi/16$

Figure: Labeling of points in the square $[-0.5, 0.5]$ embedded in the computational square $[-1, 1] \times [-1, 1]$ after rotation. (a) at position $\theta = 0$, (b) $\theta = \pi/16$.

Consistency under grid rotation, cont.

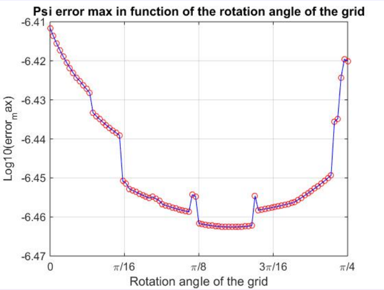

(a) ψ error after rotation

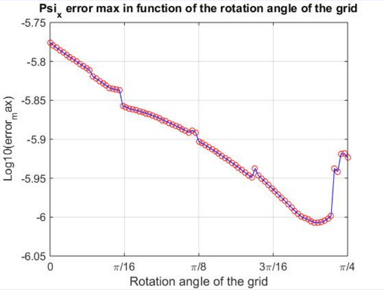

(b) ψ_x error after rotation

Figure: Maximum error for the Navier-Stokes equation in the square with size $[-0.5, 0.5] \times [-0.5, 0.5]$ embedded in $[-1, 1] \times [-1, 1]$. The exact solution is $\psi(t, x, y) = (x^2 + y^2)\exp(-t)$. The grid is 20×20. The final time $T_f = 0.25$ is reached in 20 iterations. The same computation is repeated 91 times on the domain rotated with angle $\theta = \frac{k}{90}\frac{\pi}{4}$ for $k = 0, ..., 90$.

- Left panel: accuracy for $\psi(t, x, y)$ at time $T_f = 0.25$ on the grid k.
- Right panel: accuracy for $\psi_x(t, x, y)$ at final time on the grid k. The accuracy for ψ_y is the same than the one for ψ_x.

Consistency under grid rotation, cont.

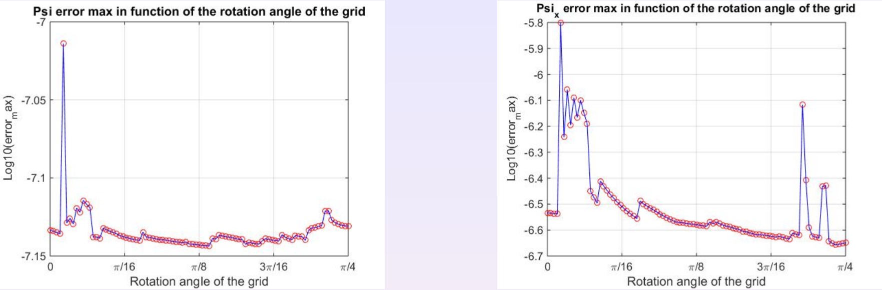

(a) ψ error after rotation

(b) ψ_x error after rotation

Figure: Maximum error for the Navier-Stokes equation in the square with size $[-0.5, 0.5] \times [-0.5, 0.5]$ embedded in $[-1, 1] \times [-1, 1]$. The exact solution is $\psi(t, x, y) = (x^2 + y^2)\exp(-t)$. The grid is 30×30. The final time $T_f = 0.25$ is reached in 20 iterations. The same computation is repeated 91 times on the domain rotated with angle $\theta = \frac{k}{90}\frac{\pi}{4}$ for $k = 0, ..., 90$.

- Left panel: accuracy for $\psi(t, x, y)$ at time $T_f = 0.25$ on the grid k.
- Right panel: accuracy for $\psi_x(t, x, y)$ at final time on the grid k. The accuracy for ψ_y is the same than the one for ψ_x.

Approximate biharmonic spectral problems in two dimensions

Let $\Omega \subset \mathbb{R}^2$. We consider the two following eigenproblems in Ω
Problem 1: The "buckling plate" problem

$$\Delta^2 \psi = \lambda(-\Delta\psi), \quad \boldsymbol{x} \in \Omega. \tag{38}$$

Problem 2: The "clamped plate" problem

$$\Delta^2 \psi = \lambda\psi, \quad \boldsymbol{x} \in \Omega. \tag{39}$$

In each case, we want to calculate approximations of the $(\lambda_n, \psi_n(\boldsymbol{x}))$, $n \geq 1$, the eigenvalues of the problem which are ordered in ascending order.

Approximate biharmonic spectral problem 1 $\Delta^2\psi = \lambda(-\Delta\psi)$ in a square

N	$\lambda_1(N)$ our scheme	$\lambda_1(N)$ (Brenner-Monk-Sun)
10	52.316494	55.4016
20	52.343018	53.2067
40	52.344588	52.5757
80	52.344685	52.4045

The reference value obtained by (Bjørstad and Tjøstheim) (1999) in the square is

$$\lambda_1 = 52.34469116841654453870533075036 5 \quad (40)$$

Relative error with the grid 80×80:

- Compact scheme: $1.18.10^{-7}$
- FEM method: $1.15.10^{-3}$

Approximate biharmonic spectral problems for Problem 1 $\Delta^2\psi = \lambda(-\Delta\psi)$ in a square

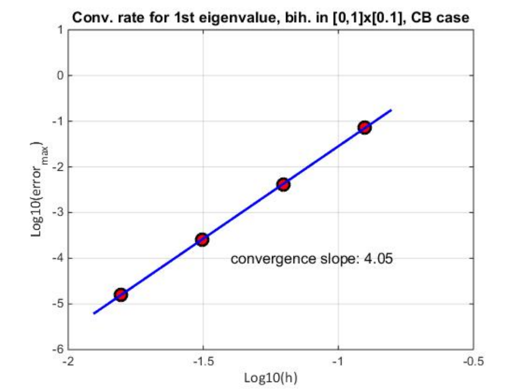

Figure: Convergence rate for the spectral Problem 1 $\Delta^2\psi = \lambda(-\Delta\psi)$

Approximate biharmonic spectral problem for Problem 2 $\Delta^2\psi = \lambda\psi$ in a square

N	$\lambda_1(N)$ by (7)	$\lambda_1(N)$ (Brenner-Monk-Sun)
10	1295.434650	1377.1366
20	1294.973270	1318.5091
40	1294.436592	1301.3047
80	1294.934146	1296.5904

The value obtained by Bjørstad and Tjøstheim (1999) in the square is

$$\lambda_1 = 1294.9339795917128081703026479744...$$

Relative error with the grid 80×80:

- Compact scheme: $1.29.10^{-7}$
- FEM method: $1.30.10^{-3}$

Approximate biharmonic spectral problems for Problem 2 $\Delta^2\psi = \lambda\psi$ in a square

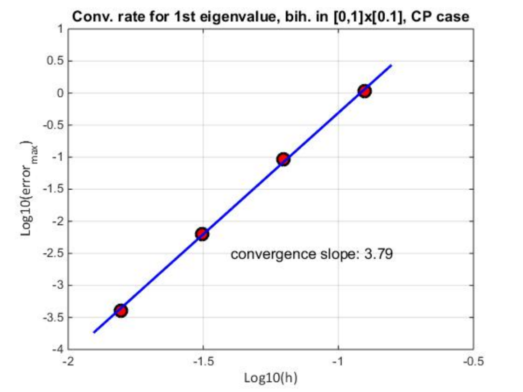

Figure: Convergence rate for the Problem 2 $\Delta^2\psi = \lambda\psi$.

Eigenfunctions for Problem 2 $\Delta^2\psi = \lambda\psi$ in a disc $x^2 + y^2 \le 1$

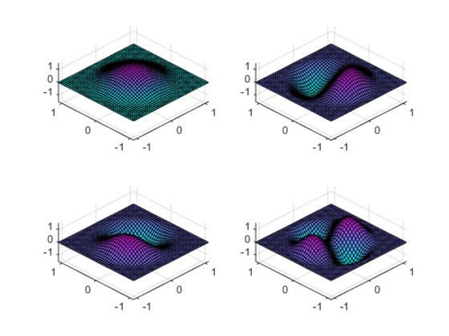

Figure: Eigenfunctions for λ_1, λ_2, λ_3, λ_4 for Problem 2 in the disc. The size of the grid is 40×40.

Eigenfunctions for Problem 2 $\Delta^2\psi = \lambda\psi$ in a disc $x^2 + y^2 \leq 1$

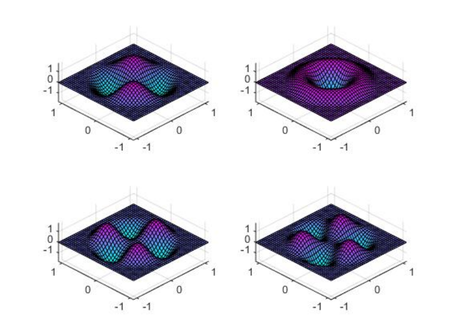

Figure: Eigenfunctions for λ_5, λ_6, λ_7, λ_8 for Problem 2 in the disc. The size of the grid is 40×40.

Eigenfunctions for Problem 2 $\Delta^2\psi = \lambda\psi$ in a disc $x^2 + y^2 \leq 1$

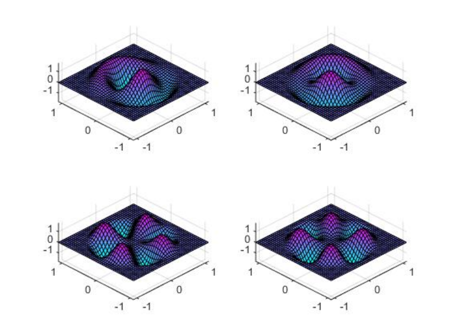

Figure: Eigenfunctions for λ_9, λ_{10}, λ_{11}, λ_{12} for Problem 2 in the disc $x^2 + y^2 \leq 1$. The size of the grid is 40×40.

Eigenfunctions for Problem 2 $\Delta^2\psi = \lambda\psi$ in a disc $x^2 + y^2 \leq 1$

N	$\lambda_1(N)$	$\lambda_2(N)$	$\lambda_3(N)$	$\lambda_4(N)$
10	0.1043056(3)	0.4510779(3)	0.4510779(3)	1.2105913(3)
20	0.1043621(3)	0.4519756(3)	0.4519756(3)	1.2159930(3)
40	0.1043630(3)	0.4520028(3)	0.4520028(3)	1.2163867(3)
80	0.1043631(3)	0.4520044(3)	0.4520044(3)	1.2164070(3)

Table: Disk $x^2 + y^2 \leq 1$ embedded in the square $[-1.1, 1.1] \times [-1, 1]$. Approximate value of the four smallest eigenvalues of the clampled plate eigenproblem (39) for $h = 1/10, 1/20, 1/40$ and $1/80$.

Eigenfunctions for Problem 2 $\Delta^2\psi = \lambda\psi$ in the ellipse $x^2/0.7^2 + y^2/1.3^2 \leq 1$

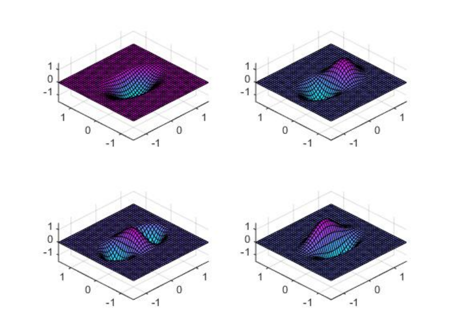

Figure: Eigenfunctions for λ_1, λ_2, λ_3, λ_4 for Problem 2 in the ellipse $x^2/0.7^2 + y^2/1.3^2 \leq 1$ embedded in $[-1.6, 1.6] \times [-1.6, 1.6]$. The size of the grid is 40×40.

Eigenfunctions for Problem 2 $\Delta^2\psi = \lambda\psi$ in the ellipse $x^2/0.7^2 + y^2/1.3^2 \leq 1$

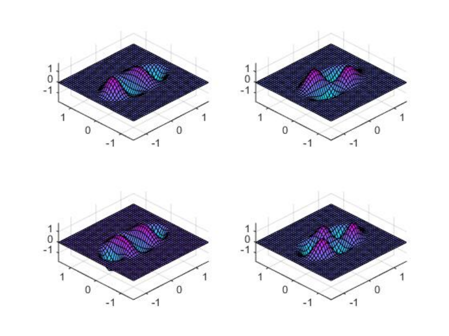

Figure: Eigenfunctions for λ_5, λ_6, λ_7, λ_8 for Problem 2 in the ellipse $x^2/0.7^2 + y^2/1.3^2 \leq 1$ embedded in $[-1.6, 1.6] \times [-1.6, 1.6]$. The size of the grid is 40×40.

Eigenfunctions for Problem 2 $\Delta^2\psi = \lambda\psi$ in the ellipse $x^2/0.7^2 + y^2/1.3^2 \leq 1$

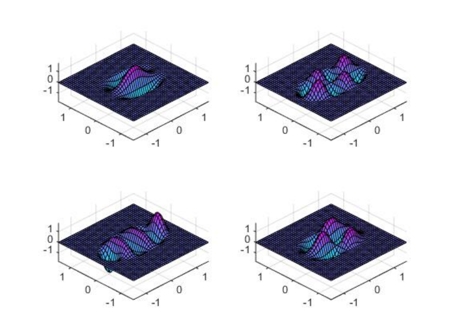

Figure: Eigenfunctions for λ_9, λ_{10}, λ_{11}, λ_{12} for Problem 2 in the ellipse $x^2/0.7^2 + y^2/1.3^2 \leq 1$ embedded in $[-1.6, 1.6] \times [-1.6, 1.6]$. The size of the grid is 40×40.

Convergence of eigenvalues for Problem 2 $\Delta^2\psi = \lambda\psi$ in the ellipse

N	$\lambda_1(N)$	$\lambda_2(N)$	$\lambda_3(N)$	$\lambda_4(N)$
10	0.2031296(3)	0.4525390(3)	0.9525603(3)	1.2572786(3)
20	0.2038618(3)	0.4531441(3)	0.9561893(3)	1.2995270(3)
40	0.2038890(3)	0.4531487(3)	0.9564064(3)	1.3003232(3)
80	0.2038902(3)	0.4531510(3)	0.9564114(3)	1.3004021(3)

Table: Ellipse $x^2/0.7^2 + y^2/1.3^2 \leq 1$ embedded in the square $[-1.6, 1.6] \times [-1.6, 1.6]$. Approximate value of the four smallest eigenvalues of the clampled plate eigenproblem (39) for $h = 1/10, 1/20, 1/40$ and $1/80$.

The eigenvalue for Problem 2 $\Delta^2\psi = \lambda\psi$, ellipse case, (cont.)

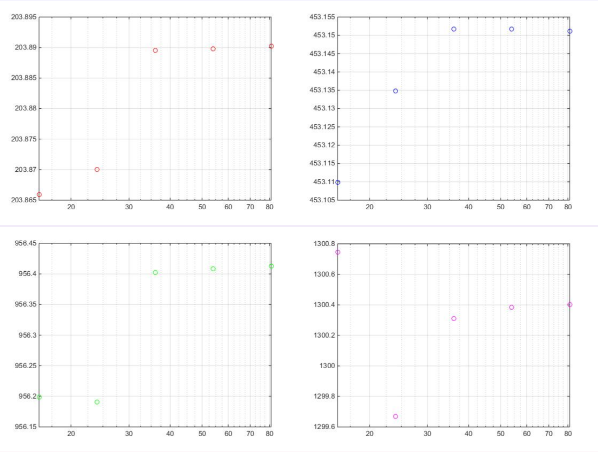

Figure: Spectral Clamped Plate problem in the ellipse $x^2/0.7^2 + y^2/1.3^2 \leq 1$. The embedding square is $[-1.6, 1.6] \times [-1.6, 1.6]$. Convergence of the eigenvalues $\lambda_1, \lambda_2, \lambda_3, \lambda_4$ with grids $N = 16, 24, 36, 54$ and 81. The

Ongoing work

- Stability analysis of the Navier-Stokes equation (streamfunction form) in domains of various shapes

$$\partial_t \Delta\psi(t,\mathbf{x}) + \nabla^{\perp}\psi.(\Delta\nabla)\psi(t,\mathbf{x}) - \nu\Delta^2\psi(t,\mathbf{x}) = \mathbf{f}(t,\mathbf{x}) \qquad (41)$$

- Convergence proof of the approximate spectrum towards the continuous spectrum in 2D, (available in 1D).

• J. W. Stephenson: Single cell discretizations of order two and four for biharmonic problems, *J. Comp. Phys.*, 55, 1984, 65–80

• E.B. Davies: *Spectral Theory and Differential Operators*, Cambridge Univ. Press, 1995.

• P.E. Bjørstad and B.P. Tjøstheim: Efficient algorithms for solving a fourth order equation with the spectral Galerkin method, *SIAM J. Sci. Comp.*, 18(2)(1997)

• M. Ben-Artzi, I. Chorev, J-P. Croisille and D. Fishelov: A compact difference scheme for the biharmonic equation in planar irregular domains", *SIAM J. Numer. Anal.*, 47, 2009, 3087–3108.

• M. Ben-Artzi, J-P. Croisille and D. Fishelov: An embedded compact scheme for biharmonic problems in irregular domains, Adv. Comp. in Indust. Math., Springer, 2018.

• M. Ben-Artzi and G. Katriel: Spline functions and the discrete biharmonic operator, *Num. Math., 2019*.